

EdgeSAM: Prompt-In-the-Loop Distillation for On-Device Deployment of SAM

Chong Zhou¹ Xiangtai Li¹ Chen Change Loy¹ ✉ Bo Dai²

¹S-Lab, Nanyang Technological University ²Shanghai Artificial Intelligence Laboratory

<https://mmlab-ntu.github.io/project/edgesam/>

Abstract

This paper presents EdgeSAM, an accelerated variant of the Segment Anything Model (SAM), optimized for efficient execution on edge devices with minimal compromise in performance. Our approach involves distilling the original ViT-based SAM image encoder into a purely CNN-based architecture, better suited for edge devices. We carefully benchmark various distillation strategies and demonstrate that task-agnostic encoder distillation fails to capture the full knowledge embodied in SAM. To overcome this bottleneck, we include both the prompt encoder and mask decoder in the distillation process, with box and point prompts in the loop, so that the distilled model can accurately capture the intricate dynamics between user input and mask generation. To mitigate dataset bias issues stemming from point prompt distillation, we incorporate a lightweight module within the encoder. EdgeSAM achieves a 40-fold speed increase compared to the original SAM, and it also outperforms MobileSAM, being 14 times as fast when deployed on edge devices while enhancing the mIoUs on COCO and LVIS by 2.3 and 3.2 respectively. It is also the first SAM variant that can run at over 30 FPS on an iPhone 14.

1. Introduction

In this study, we explore the feasibility of deploying the Segment Anything Model (SAM) [23] directly on edge devices, such as smartphones, to enable real-time interactive segmentation and facilitate its integration in various downstream tasks. Addressing this challenge is non-trivial. First, SAM was not designed for on-device deployment. It has a total parameter count of 641M and requires 2735 GFLOPs under its fixed 1024×1024 input resolution. Without any specialized optimization, we failed to run SAM on an iPhone 14 due to its large computation and memory consumption. Even on an NVIDIA 2080 Ti, the throughput is just four images per second.

A seemingly straightforward solution to enhance speed is to replace SAM’s huge ViT-based image encoder with a more compact version, as demonstrated by Mobile-

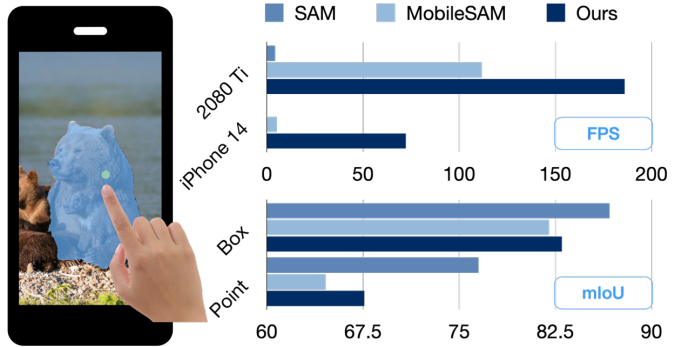


Figure 1. EdgeSAM is the first SAM variant that runs at over 30 FPS on mobile platforms. Here, we show its encoder throughput compared with SAM and MobileSAM as well as the mIoU performance on the SA-1K dataset with box and point prompts.

SAM [58]. This approach indeed leads to a considerable speed increase, approximately 26 times faster, but it also substantially reduces the performance. For instance, the mask mIoU on the COCO dataset [28] drops from 77.3 to 74.5 with the ground-truth boxes as the box prompts. Moreover, when deployed on edge devices, the speed of MobileSAM is still far from being real-time. For example, on iPhone 14, its throughput is only five images per second.

To mitigate the performance degradation and step further towards the real-time inference on edge devices, we propose EdgeSAM, which runs over 30 FPS on iPhone 14 with comparable accuracy to the original SAM. Our key insight is to consider prompts during knowledge distillation so that the student model receives task-specific guidance and focuses on harder training targets, such as a finer boundary.

In our extensive empirical investigations, it became unexpectedly clear that the key factor in knowledge distillation is not the incorporation of losses specifically tailored for dense tasks [31, 43] or query-based detectors [4, 6, 20]. Rather, it is the strategic selection of prompts during the distillation process that holds paramount importance. Addressing this, we introduce a novel approach: a dynamic *prompt-in-the-loop* strategy. This technique effectively enables the student model to assimilate the intricate knowl-

edge encapsulated within SAM. It involves actively aligning the student model with the multi-grained output masks of SAM and iteratively introducing new prompts in regions where the student model exhibits inaccuracies. These tailored prompts guide the mask decoder, emphasizing areas of incorrect segmentation, thereby enhancing the learning process. Furthermore, we investigated various training configurations, examining different types of prompts, the impacts of freezing encoder/decoder components, and the selection of distillation targets. The specifics and findings of these explorations are detailed in the experimental section.

Additionally, we conducted thorough ablation studies focusing on the selection of the backbone architecture, particularly in view of the throughput-performance balance crucial for on-device deployment. We find that purely CNN-based architectures emerge as the more advantageous choice to ViT-based backbones for achieving the optimal trade-off. This is attributed to the current landscape of on-device AI accelerators, such as Apple Neural Engine (ANE), which are predominantly optimized for CNNs rather than ViT architectures. This observation also underscores the versatility of our proposed prompt-aware knowledge distillation approach, highlighting its applicability across diverse architectures.

In our final observations, we note that SAM, having been trained on a dataset with multi-grained annotations, encounters challenges in resolving the granularity of output when faced with ambiguous prompts, such as a single point. This is particularly evident when SAM is prompted with center points on the COCO dataset during evaluations; the model does not consistently produce instance-level masks, but rather part-level masks. This issue becomes more pronounced when SAM functions as the teacher model. To address this, we propose a simple yet effective module designed to explicitly discern and adapt to the granularity priors specific to a given test set or application scenario. This module enhances SAM’s ability to accurately interpret and respond to varying levels of prompt ambiguity.

Consequently, our EdgeSAM model achieves a remarkable performance boost, operating *40 times* faster than the original SAM and *1.6 times* more swiftly than MobileSAM on an NVIDIA 2080 Ti GPU. Notably, on the iPhone 14, EdgeSAM leverages its purely CNN-based backbone [49] to process image encoding in a mere 14 ms per image. This rate is *14 times faster* compared to MobileSAM’s performance on the same platform. Even when combined with the mask decoder, EdgeSAM maintains an overall speed exceeding 30 FPS, marking it as the first SAM variant capable of real-time operation on edge devices. In terms of accuracy, EdgeSAM closely parallels the original SAM in box-prompt performance across the SA-1B [23], COCO [28], and LVIS [11] datasets. Additionally, it surpasses MobileSAM by an average of 2 mAP and 2-3 mIoU in point-

prompt performance across these datasets. This capability to run SAM in real-time on edge devices opens up a multitude of possibilities for downstream applications, including on-device video editing and video instance segmentation.

2. Related Work

Efficient Model Design. This research direction mainly focuses on designing efficient CNNs [12, 16, 17, 22, 34, 42, 62], transformers [35, 36, 39], and their mixed architecture [7, 24, 33, 59], with the goal of visual representation learning. Our work also adopts efficient models as the image encoder but is orthogonal to these works as it can be applied to various efficient backbones.

Knowledge Distillation in Detection and Segmentation. The majority of research in knowledge distillation has been centered on classification tasks [10, 13, 54, 57, 63]. Several studies [31, 43, 50, 51, 53, 60] have applied knowledge distillation techniques to dense prediction tasks like semantic segmentation and object detection. Common approaches in these works involve leveraging pixel-wise correlations or channel-wise interactions between dense features of teacher and student models. Recently, there has been an increased interest in developing specialized knowledge distillation losses for query-based detectors such as DETR [3], as evidenced by works like [4, 6, 20]. MobileSAM [58], closely related to our work, implements pixel-wise feature distillation between the SAM encoder and a compact backbone. However, it does not address the prompt encoder and mask decoder, leading to a significant performance discrepancy compared to the original SAM. FastSAM [65], on the other hand, trains a YOLACT-based [1] instance segmentation model using the SA-1B dataset and employs heuristic rules for post-process object selection, a method that aligns marginally with the SAM principles.

Efficient Segmentation Models. Prior studies in efficient segmentation [14, 15, 19, 25, 26, 37, 38, 48, 55, 56, 64] have predominantly concentrated on close-set segmentation within specific domains, with a significant portion of this research [19, 25, 38] specifically targeting driving scenarios. More recently, a few works [48, 61] have ventured into designing segmentation models suitable for on-device implementation, capable of running efficiently on mobile platforms. However, the realm of on-device interactive segmentation remains largely unexplored. MobileSAM [58] represents an initial attempt, but it still encounters challenges regarding computational efficiency and a noticeable decline in performance, indicating a substantial opportunity for further advancements in this direction.

3. Method

In this section, we first briefly introduce SAM (Sec. 3.1), followed by our proposed method, EdgeSAM, that slims

SAM by encoder distillation (Sec. 3.2.1), prompt-in-the-loop distillation (Sec. 3.2.2), and a lightweight module that embeds the granularity preferences (Sec. 3.2.3).

3.1. Preliminaries: SAM

The SAM model consists of three components: image encoder, prompt encoder, and mask decoder. In particular, the image encoder takes up the most computational cost and parameters. It follows the backbone design of ViTDet [27], which essentially is a hierarchical vision transformer. The input and output sizes of the image encoder are kept fixed at (3, 1024, 1024) and (256, 64, 64).

SAM can handle four types of prompts, including point, box, mask, and text. Points and boxes are considered as the sparse prompts, which are encoded with random positional embeddings [47] summed with a type indicator token. Masks and free-form texts are embedded with a tiny CNN and the text encoder of CLIP [40], respectively. In this paper, we focus on the point and box prompts.

The mask decoder takes as input the image feature, embedded point and/or box prompts, mask prediction tokens, and an IoU prediction token. All the inputs will be mixed and encoded with a lightweight two-way transformer. As a result, each mask token is transformed into a dynamic linear classifier, which can compute the foreground probability of each spatial location of the image feature. The IoU token yields the mask confidence score for each mask.

Apart from the interactive prompt-based model design, the SA-1B dataset also contributes significantly to SAM’s zero-shot generality. It is the largest segmentation dataset to date, with over 1 billion mask annotations across 11 million images. Here, we highlight several characteristics of SA-1B to better understand SAM’s capabilities: (1) the mask annotations are obtained by prompting an ambiguity-aware model, that is trained on semi-automatically labeled data, with grid points; (2) the masks are class-agnostic; (3) and the annotations are multi-grained in both instance and part levels. As we will discuss later, those properties of SA-1B make distillation on SAM different and more challenging than previous segmentation models.

3.2. EdgeSAM

The goal of EdgeSAM is to transfer the capabilities of SAM into a much more compact model, which makes deployment on edge devices feasible. In particular, as shown in Fig. 2, EdgeSAM maintains the encoder-decoder architecture of SAM and aims to preserve the performance of zero-shot interactive segmentation with box and point prompts. We train EdgeSAM with only 1% data from the SA-1B dataset and evaluate its zero-shot transferability on the COCO [28] and LVIS [11] datasets.

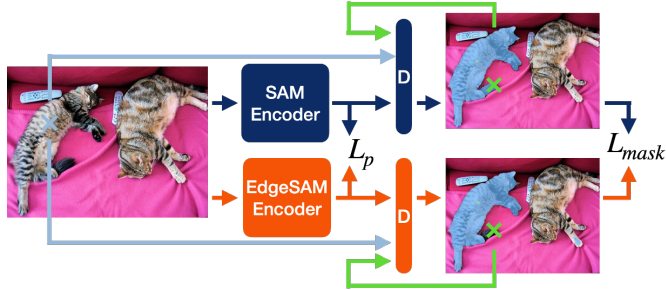


Figure 2. **Overview of EdgeSAM.** We first apply encoder-only KD between the output feature of the image encoder of SAM and EdgeSAM. Then we adopt prompt-in-the-loop KD, which interactively samples point prompts from the wrongly segmented areas. Note that, the initial prompt can also be a box.

3.2.1 Encoder-Only Knowledge Distillation

Inspired by MobileSAM [58], we adopt a pixel-wise feature distillation loss L_p between the image encoder T_{enc} of SAM and an efficient network S_{enc} as follows:

$$L_p = \text{MSE}(T_{enc}(I), S_{enc}(I)), \quad (1)$$

where I denotes the input image. Since the downsampling stride and feature channels of the student model and SAM image encoder are not aligned, MobileSAM removes the downsampling operations in the last two stages of the student model and uses a projection layer to align the channel dimension. We also use the projection layer for channel alignment, but we keep the downsampling layers unchanged. Instead, we construct a tiny FPN [29] that up-samples the feature to the desired resolution and performs element-wise addition with features from previous stages.

We explore various efficient backbones following this paradigm, including ViT-based [52], CNN-based [49], and hybrid networks [2]. However, we find there is always a considerable performance gap. Training with a longer schedule or using distillation losses [31, 43] designed for dense prediction tasks does not show an obvious improvement. Therefore, we further propose to consider prompts during distillation to provide task-specific guidance.

3.2.2 Prompt-In-the-Loop Knowledge Distillation

Since the original SAM decoder is lightweight enough, taking up only 0.6% of the total parameters of SAM, we retain its architecture so that the pre-trained weights can be inherited. Here, we re-visit the mask decoder of SAM. It is a two-stream bi-directional transformer, with output feature map f from the image encoder as the input of one stream and sparse prompt embeddings p concatenating with four mask tokens m and an IoU token c as the input of the other stream¹. The sparse prompt can be any combination of pos-

¹We ignore the dense prompts and focus only on point and box prompts.

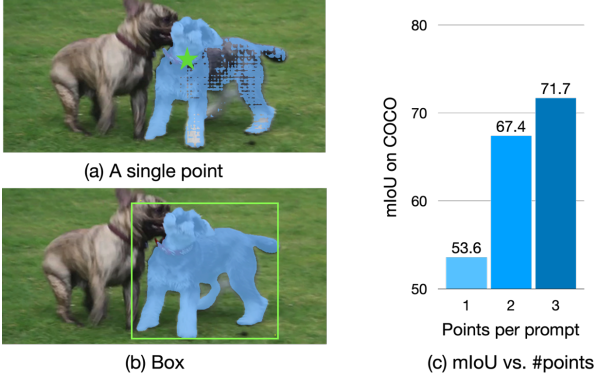


Figure 3. **Behaviors of the SAM with different prompts.** When prompting with ambiguous prompts, *e.g.*, a point, SAM yields sub-optimal results. More informative prompts solve the problem.

itive/negative points and a single box, indicating the user’s object of interest.

With these inputs, there are many potential distillation targets for teacher and student models to align with, including the refined feature map, mask/IoU tokens, cross attention between two streams of the inputs, and output mask logits. Through empirical studies, we find that supervising the student with teacher mask output as the ground truth is the most effective. More details are provided in the appendix. We formulate the decoder loss as follows:

$$L_d = L_{\text{mask}}(\phi(T_{\text{dec}}(f_t, p, m, \mathbf{c})), S_{\text{dec}}(f_s, p, m, \mathbf{c})), \quad (2)$$

where $\phi(\cdot)$ is binary thresholding, f_t and f_s denote the feature from the teacher and student image encoder, respectively. The teacher and student share the same set of p , m , and \mathbf{c} , which are kept frozen during training. We adopt a combination of the Dice loss [45] and BCE loss as the mask loss L_{mask} . Note that we allow the gradient backpropagate to the image encoder so that it is jointly learned.

While the distillation loss is frustratingly simple, the prompt selection for each training iteration needs to be carefully designed. We observe that fine-tuning the mask decoder poses a threat to the zero-shot generalization ability. That is, training with a particular combination of prompts sabotages its capability when inferencing with prompt combinations that are not used during training. For instance, training only with points leads to a significant performance drop when testing with box prompts. While freezing the mask decoder or using LoRA [18] on the decoder for regulation mitigates the problem, it also limits the performance upper-bound for prompts observed during training. Meanwhile, we find that even the original SAM outputs unsatisfactory mask predictions when prompted with ambiguous prompts, such as a single point. As shown in Fig. 3, on the COCO dataset, with the object center as the prompt, the mask mIoU of SAM is only 53.6. Thus, aligning the student’s outputs in such circumstances might not be optimal.

Algorithm 1: Prompt-In-the-Loop Distillation

```

 $T_{\text{enc}}, S_{\text{enc}} \leftarrow$  SAM / EdgeSAM encoder;
 $T_{\text{dec}} \leftarrow$  SAM decoder;
 $S_{\text{dec}} \leftarrow$  EdgeSAM decoder initialized w/  $T_{\text{dec}}$ ;
 $m, \mathbf{c} \leftarrow$  shared mask / IoU tokens;
 $\mathcal{I}, \mathcal{P} \leftarrow$  images and prompts for training;
 $N, M \leftarrow$  training steps, prompt sampling loops;
for  $i = 1, 2, \dots, N$  do
     $f_t, f_s \leftarrow T_{\text{enc}}(\mathcal{I}_i), S_{\text{enc}}(\mathcal{I}_i)$ ;
     $p \leftarrow$  select the box or point prompt in  $\mathcal{P}_i$ ;
     $m_t, m_s \leftarrow T_{\text{dec}}(f_t, p, m, \mathbf{c}), S_{\text{dec}}(f_s, p, m, \mathbf{c})$ ;
     $L \leftarrow L_{\text{mask}}(m_t, m_s)$ ;
    for  $j = 1, 2, \dots, M$  do
         $\hat{p} \leftarrow$  sample_in_disagree( $m_t, m_s$ );
         $p \leftarrow \hat{p}$  appends to  $p$ ;
         $m_t, m_s \leftarrow$ 
             $T_{\text{dec}}(f_t, p, m, \mathbf{c}), S_{\text{dec}}(f_s, p, m, \mathbf{c})$ ;
         $L \leftarrow L + L_{\text{mask}}(m_t, m_s)$ ;
    end
     $S_{\text{enc}}, S_{\text{dec}} \leftarrow$  SGD model update;

```

end

To enhance the efficacy of our distillation process, we introduce a dynamic prompt sampling strategy. This approach is designed to achieve three key objectives: (1) dynamically generate a diverse set of prompt combinations from the initial prompt (be it a box or a point), (2) accurately identify areas within the mask where the student model exhibits inaccuracies, thereby directing its focus to these specific segments, and (3) compel the teacher model, namely the SAM, to produce high-quality masks for more precise guidance.

Drawing inspiration from recent advancements in interactive segmentation methods [9, 44], our strategy involves iteratively sampling new prompts in the loop during the distillation phase. As detailed in Algo. 1, we start with an initial prompt. With equal probability, either a box or point prompt, as provided by the SA-1B dataset, is input into the decoders of both the teacher and student models. Subsequently, we identify areas where the mask predictions from the teacher and student diverge. As shown in Fig. 4, using the teacher’s output as the reference, we uniformly sample new prompts: a positive point in regions marked as false negatives, or a negative point in areas identified as false positives. These newly sampled points are then amalgamated with the existing prompts for the subsequent iteration of decoding. It is important to note that each prompt leads to four mask predictions at varying levels of granularity. In our analysis, the disagreement is calculated specifically between the teacher mask with the highest IoU score and its corresponding student mask.

In summary, our findings reveal that rather than relying on distillation with losses dedicated to dense prediction or

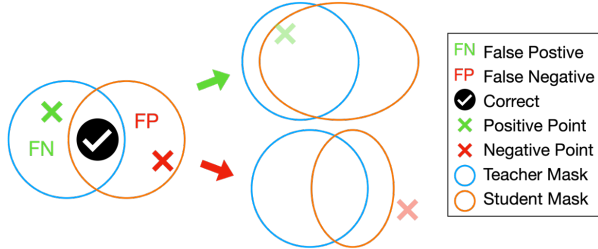


Figure 4. During distillation, we randomly sample new positive/negative point prompts from the FN/FP areas in a loop, so that the student dynamically focuses on those regions.

query-based approaches, dynamically feeding appropriate prompt combinations into the mask decoder during the distillation process proves to be more effective. Our prompt-in-the-loop distillation method prioritizes the strategic use of prompts to enhance the learning process. In the experimental section, we present detailed discussions through comprehensive ablation studies.

3.2.3 Granularity Priors

Since SA-1B is a class-agnostic, multi-grained, automatically labeled dataset, its annotation distribution can be very different from that of the datasets that are intensively labeled by human labor, such as COCO. Therefore, with ambiguous prompts, such as a single point, it is hard for SAM to determine the desired output granularity. Meanwhile, as shown in Fig. 3, with box prompts, SAM can easily pinpoint the target granularity. In addition, compared to iteratively clicking or interacting with the box, there are many circumstances and applications on smartphones that a single click is favored, such as click-and-drag. Therefore, we propose a simple and efficient module that explicitly embeds the granularity priors of certain datasets and can be optionally turned off if the original behavior of SAM is preferred.

With the image encoder staying frozen, we build a lightweight region proposal network (RPN) [41] on top of it, which consists of a feature pyramid network (FPN) [29] and a shared detection head. For efficiency, we follow the design proposed by EfficientDet [46]. The RPN is trained on a specific dataset, *e.g.*, COCO [28], to capture its granularity prior. During inference, we merge the proposal boxes whose centers are K nearest neighbors of the point prompts weighted by their confidence scores. Finally, we combine the merged box with the point input together as the prompt that inputs to the mask decoder.

3.3. Training and Application

Training Pipeline. We divide the training into three stages. In the first stage, we perform encoder-only knowledge distillation on 1% SA-1B images following MobileSAM [58].

In the second stage, we apply prompt-in-the-loop distillation on the same image set but with point and box prompts as part of the inputs. In the final stage, which is optional, we freeze modules other than the lightweight RPN and train with the class-agnostic ground-truth boxes with the commonly used focal loss [30] and Huber loss [21].

Inference and On-Device Demo. Our EdgeSAM model is capable of initiating inference with either point or box prompts, and, akin to SAM, it can progressively incorporate additional points for further refinement. To show the practical utility of EdgeSAM, we have developed an on-device demonstration. We highly recommend exploring this demo to fully appreciate EdgeSAM’s capabilities.

4. Experiments

Efficiency. We measure the model efficiency mainly by throughput per second on a single NVIDIA 2080 Ti and an iPhone 14 as it reflects the real-world latency. We also report FLOPs and total parameters for side reference.

Accuracy. We divide the accuracy measurement into three scenarios according to the prompt type and source. (1) We use the ground-truth box as the initial prompt and iteratively add more point prompts for refinement. (2) Similar to (1) but using the center point of the ground-truth mask as the initial prompt. (3) An external object detector is leveraged to provide box prompts. For (1) and (2), we calculate the mIoU across all instances, and for (3), we report mAP and boundary IoU [8]. For all evaluations, we take the output of the first mask token as the prediction.

Datasets. We consider SA-1B [23], COCO [28], and LVIS [11] to evaluate both in-domain performance and zero-shot transferability. For distillation, 1% images of the whole SA-1B dataset are used. We construct a test set, named SA-1K, from SA-1B. In particular, we randomly select 1,000 images from SA-1B, which are not used during training. For each image, we randomly sample 64 instances to avoid memory overflow. For COCO and LVIS, we use their default validation sets.

4.1. Implementation Details

As mentioned in Sec. 3.3, we split the training into three stages. In the first stage, we train on 1% of SA-1B images with encoder-only distillation loss L_p . We train the model for 10 epochs with the batch size set to 64. We adopt the AdamW optimizer [32] and set the initial learning rate to $1.25e-2$. We adopt the cosine decay schedule, which gradually decreases the learning rate to $6.25e-7$. In the second stage, we load the encoder weights trained in stage one and inherit decoder weights from SAM. We then train with the prompt-in-the-loop distillation loss L_d on 1% SA-1B for 5 epochs. The batch size is 16, and the learning rate decays from $1e-4$ to $1e-5$. We set the maximum allowed instances

Table 1. **Efficiency comparison.** For FPS, we only report the encoder FPS as all models share the same decoder which only takes 12ms per image on iPhone 14. * denotes EdgeSAM with the RPN.

Model	FPS		MParam.	GFLOPs
	2080 Ti	iPhone 14		
SAM	4.3	N/A	641.1	2734.8
MobileSAM	111.7	5.2	9.8	38.2
EdgeSAM	185.9	72.3	9.6	22.1
EdgeSAM*	135.8	57.8	9.8	22.2

Table 2. **Performance with GT boxes as prompts.** We report the mIoU across all instances in the test set. +1 pt. denotes appending an additional refinement point as the prompt. **Bold** marks the best while underline marks the second best.

Method	SA-1K			COCO			LVIS
	Box	+1 pt.	+2 pt.	Box	+1 pt.	+2 pt.	Box
SAM	86.7	86.7	87.1	77.3	<u>77.7</u>	<u>78.1</u>	77.5
MobileSAM	82.0	82.4	82.7	74.4	74.8	75.1	72.8
EdgeSAM	<u>83.0</u>	<u>83.7</u>	<u>84.1</u>	<u>76.7</u>	78.1	79.0	<u>76.0</u>

per image to 16, and the number of loops for prompt sampling is 1. In the final optional stage for RPN training, we follow the 1x schedule of MMDetection [5] on COCO [28].

4.2. Quantitative Results

Efficiency. In Tab. 1, we compare the encoder FPS of SAM, MobileSAM, and EdgeSAM on both the desktop and mobile platforms. When evaluating with NVIDIA 2080 Ti, we compile the models with ONNX to avoid the overhead of the Python interpreter, and we make sure the GPU is running at 100% payload. On iPhone 14, we use the Core ML Tools as the compiler and measure the throughput with the benchmark tools provided by Xcode. As shown in Tab. 1, the proposed EdgeSAM is significantly faster than SAM and MobileSAM, especially on the mobile platform. In particular, the encoder of EdgeSAM is *over 40 times faster* than SAM on NVIDIA 2080 Ti and approximately *14 times faster* than MobileSAM on iPhone 14. From the benchmark report, we observe that MobileSAM is not well optimized by on-device AI accelerators, such as ANE, which explains the vast differences between desktop and mobile platforms. In addition, combined with the decoder, which takes 12 ms per run, the EdgeSAM delivers an overall *38 FPS* speed on an iPhone 14, which makes it the first SAM variant running in real-time on edge devices. More comparisons can be found in Appendix A.

Prompting with GT Boxes. Despite being extremely lightweight, EdgeSAM can generate accurate segmentation masks. As shown in Tab. 2, the proposed EdgeSAM consistently outperforms MobileSAM across a wide range of prompt combinations and datasets, demonstrating its effectiveness for real-world applications, including zero-shot

Table 3. **Performance with center points as prompts.** Similar to Tab. 2 but using the mask center point as the initial prompt. * denotes using RPN for granularity priors.

Method	SA-1K			COCO			LVIS
	Center	+1 pt.	+2 pt.	Center	+1 pt.	+2 pt.	Center
SAM	76.5	83.4	85.1	53.6	67.4	71.7	60.0
MobileSAM	64.6	73.4	76.2	<u>50.9</u>	<u>63.0</u>	66.8	51.4
EdgeSAM	<u>67.5</u>	<u>76.1</u>	<u>79.0</u>	48.0	61.8	<u>68.7</u>	<u>53.5</u>
EdgeSAM*				54.3			

Table 4. **Performance with boxes from an external object detector as prompts.** We report the mask mAP and boundary IoU on the COCO dataset. The box mAP of the object detector is 47.4.

Method	AP	AP _S	AP _M	AP _L	BIoU
SAM	38.8	26.9	44.1	50.3	26.8
MobileSAM	33.1	21.7	37.8	44.8	20.2
EdgeSAM	<u>35.2</u>	<u>23.5</u>	<u>40.3</u>	<u>46.6</u>	<u>22.5</u>

transferability and iterative refinement. To our surprise, on the COCO dataset, with one or two points serving as the refinement prompts, EdgeSAM even surpasses the SAM.

Prompting with Center Points. Similar to prompting with GT boxes, EdgeSAM shows a clear advantage over MobileSAM in most cases, as shown in Tab. 3. However, as we have discussed in Sec. 3.2.3, with ambiguous prompts, such as a single point, the original SAM does not always produce masks in the desired granularity. In addition, EdgeSAM is trained on the SA-1B dataset, whose granularity distribution is very different from that of COCO. Therefore, with the proposed task-aware distillation, EdgeSAM is more likely to fit the SAM granularity distribution when handling ambiguous prompts than MobileSAM. To explicitly capture such a granularity prior, we propose a lightweight RPN, which works as expected and makes the single point performance on COCO rise from 48.0 to 54.3.

Prompting with External Object Detectors. We finally combine all the SAM variants with an external object detector (We use Detic [66] from MMDetection [5]) and evaluate their mAP performance on COCO. This setting examines a practical use case where automatic segmentation is preferred over interactive segmentation, *e.g.*, generating the mask within the tracking box. We use an object detection framework to generate bounding boxes and associated class labels, ensuring that the observed variations in mAP are attributed solely to the quality of the masks generated. This approach also evaluates the resilience of our model in handling imprecise bounding box inputs. We also report boundary IoU [8] to reflect the boundary accuracy. Table 4 shows that while EdgeSAM outperforms MobileSAM by considerable margins, it lags behind SAM. This performance gap may reflect not only inherent limitations in model capacity but also a consequence of training exclusively with ground-

Table 5. **Ablation studies.** If not explicitly stated, we report the mIoUs on SA-1K. For more ablation studies, please refer to Appendix B.

(a) Effectiveness of prompt-in-the-loop knowledge distillation (KD).						
Method	Box	+1 Pt.	+2 Pt.	Center	+1 Pt.	+2 Pt.
encoder-only KD	82.0	82.4	82.8	64.6	73.3	76.2
+ prompt-in-the-loop KD	83.0	83.7	84.1	67.5	76.1	79.0

(b) Speed-performance trade-off of the RPN for granularity priors.			
Evaluated on COCO with center point as the prompt. We report the FPS on NVIDIA 2080 Ti and iPhone 14.			
Method	mIoU	2080 Ti	iPhone 14
w/o RPN	48.0	185.9	72.3
w/ RPN	54.3	135.8	57.8

(c) Choice of the backbone. We apply encoder-only KD for this ablation. FPS is measured on a single NVIDIA 2080 Ti with the decoder excluded.					
Method	Res. Align	Type	Box	Center	FPS
TinyViT-5M	Remove Downsample	ViT	82.0	64.6	111.7
EfficientViT-B1		Hybrid	81.6	63.7	127.6
RepViT-M1		CNN	82.1	64.9	175.0
TinyViT-5M	FPN	ViT	81.6	63.7	124.2
EfficientViT-B1		Hybrid	80.7	60.9	180.3
RepViT-M1		CNN	82.0	64.6	185.9

(e) Number of prompt sampling loops.						
Loops	Box	+1 Pt.	+2 Pt.	Center	+1 Pt.	+2 Pt.
0	83.1	83.2	83.4	67.4	71.1	72.4
1	83.0	83.7	84.1	67.5	76.1	79.0
2	82.9	83.7	84.1	67.3	76.1	79.2

(d) Frozen modules and LoRA [18]. F denotes freezing and L means applying LoRA during training.					
Encoder	Decoder	SA-1K		COCO	
		Box	Center	Box	Center
F	-	82.3	65.7	76.4	47.4
-	F	83.5	67.7	75.9	48.3
-	L	82.9	66.8	74.9	46.8
-	-	83.1	67.4	76.7	48.2

(f) Training stages.			
	Box	Center	
Joint	81.2	63.2	
Two-stage	83.1	67.4	

(g) Encoder-only KD.		
Method	Box	Center
Baseline	82.0	64.6
20 Epochs	81.9	65.9
w/ Structured [31]	81.6	65.2
w/ Channel-wise [43]	81.8	64.9

truth boxes, which could lead to discrepancies during inference. Addressing these differences and exploring their implications is a promising direction for future research.

4.3. Ablation Studies

Effectiveness of Each Proposed Component. We investigate the effectiveness of the introduced techniques, namely, prompt-in-the-loop knowledge distillation (prompt-KD) and the lightweight Region Proposal Network (RPN) that incorporates granularity priors. As depicted in Tab. 5a, prompt-KD demonstrates a notable enhancement in performance over encoder-only knowledge distillation, particularly when complemented with additional refinement points. Prompt-KD’s advantage lies in its provision of task-specific supervision, which is more explicit and targeted than the general guidance offered by encoder-only KD. In addition, its strategy of dynamically generating new prompts in inaccurately segmented areas places more focus on these regions, creating diverse prompt combinations in the process. Furthermore, as shown in Tab. 5b, the lightweight RPN operates effectively at a manageable computational cost. It is important to note that during the RPN’s training phase, we freeze the other components, including the backbone network. This approach allows for the RPN to be dynamically deactivated during inference, ensuring that the model’s generalization capabilities remain intact.

Choice of the Backbone. As mentioned in Sec. 3.2.1, the output resolution of SAM and that of efficient back-

bones are misaligned. MobileSAM proposed to remove the downsampling operations in the last several stages, while we experiment with fusing low-resolution feature maps with higher ones through an FPN [29]. In addition, we compare the performance-speed trade-offs across efficient backbones following the ViT-based [52], CNN-based [49], and hybrid [2] designs. As shown in Tab. 5c, the purely CNN-based RepViT-M1 with FPN for resolution alignment achieves the best balance. Moreover, as many on-device AI accelerators, such as ANE, are highly optimized for CNNs, the speed gap becomes larger when deployed on edge devices. For example, on iPhone 14, with FPN for resolution alignment, RepViT-M1 only takes 14 ms to encode a 1024×1024 input, which is 14x and 4x faster than TinyViT-5M and EfficientViT-B1 respectively. Therefore, our EdgeSAM adopts it as the image encoder.

Other Ablations. In Tab. 5d, we test several configurations regarding module freezing and LoRA [18]. In particular, LoRA is applied to the query and value projection layers of the attention blocks in the decoder. Results show that freezing the decoder during distillation yields the best in-domain accuracy while fine-tuning all the modules generalizes better on other datasets. To benefit more practical settings, we opt to fine-tune both the encoder and decoder. Furthermore, we vary the number of prompt sampling loops during distillation, in Tab. 5e, we find one additional loop is good enough, thus setting the loop number to be 1 by default. In addition, due to the optimal



Figure 5. **Qualitative results of EdgeSAM with point and box prompts.** The green and red stars indicate the positive and negative points respectively. More comparative results between EdgeSAM and SAM are provided in Appendix C.

optimization settings being different for encoder-only distillation and prompt-in-the-loop distillation, we find joint-training yields sub-optimal results compared to training in two stages (see Tab. 5f). Therefore, we propose to train them sequentially. Finally, in Tab. 5g, we explore several ways to improve the performance of encoder-only distillation, including training for a longer schedule and applying knowledge distillation losses designed for dense prediction tasks [31, 43]. While they boost the performance of point prompts, that of box prompts slightly drops, indicating an upper-bound performance of encoder-only distillation. This motivates us to explore prompt-aware distillation.

4.4. Qualitative Results

In Fig. 5, we visualize the mask quality of EdgeSAM with one point, two points, and one box as the prompts, respectively. Note that *none* of the images are from the SA-1B dataset that EdgeSAM is trained on, demonstrating its zero-shot generalization ability. We provide more visual comparisons between SAM and EdgeSAM in Appendix C. We also implement an on-device demonstration application that showcases more qualitative results of EdgeSAM. We highly suggest exploring this demo for a better understanding of EdgeSAM’s capabilities and applications.

5. Conclusion

In this paper, we present EdgeSAM, the first SAM variant that runs in real-time on edge devices. We achieve this by

distilling SAM into a lightweight CNN-based architecture. Our preliminary experiments show that existing distillation schemes, that only involve the image encoder thus being task-agnostic, fail to reveal the full knowledge spectrum of SAM to the student model. Thus, we propose a prompt-in-the-loop knowledge distillation method that considers both the encoder and decoder of SAM and provides task-specific supervision signals. Experiments across SA-1B, COCO, and LVIS under various settings demonstrate the effectiveness of EdgeSAM in terms of efficiency and accuracy compared with SAM and MobileSAM.

Despite being able to run EdgeSAM at a decent speed on edge devices, we still have several research directions, that could potentially provide boosts, left to be investigated, including quantization, model pruning, on-device optimization, mixed-precision inference, *etc.* Besides, we haven’t applied any augmentation during training, thus proper data or prompt augmentation might also be promising directions. We hope EdgeSAM will encourage more real-world applications with its on-device interactive segmentation capability and will continue working on further improvements.

Acknowledgments. This study is supported under the RIE2020 Industry Alignment Fund Industry Collaboration Projects (IAF-ICP) Funding Initiative, as well as cash and in-kind contribution from the industry partner(s). We are grateful to Han Soong Chong for his effort in the demonstration application.

Table 6. **Performance with boxes prompts.** We report the mask mAP on the COCO dataset. ViTDet-H [27] is used as the detector, whose box mAP is 58.7, to provide box prompts. For speed benchmarking, we infer both the encoder and decoder (instead of encoder-only). Thus, the numbers are different from those in the main paper. FLOPs are calculated based on the 1024×1024 input resolution. Numbers denoted by * are copied from MobileSAM [58]. 3x and 10x represent training with more data. **Bold** marks the best while underline marks the second best.

Method	Train Set	COCO				GFLOPs	MParam.	FPS		
		AP	AP _S	AP _M	AP _L			iPhone 14	2080 Ti	3090
SAM [23]	SA-1B	46.1	33.6	51.9	57.7	2734.8	641.1	-	4.3	-
FastSAM [65]	2% SA-1B	37.9	23.9	43.4	50.0	887.6	68.2	-	-	<u>25.0*</u>
MobileSAM [58]	1% SA-1B	39.4	26.9	44.4	52.2	<u>38.2</u>	9.8	<u>4.9</u>	<u>103.5</u>	100.0*
EdgeSAM (Ours)	1% SA-1B	<u>42.2</u>	<u>29.6</u>	<u>47.6</u>	<u>53.9</u>	22.1	9.6	38.7	164.3	-
EdgeSAM-3x	3% SA-1B	42.7	30.0	48.6	54.5	22.1	9.6	38.7	164.3	-
EdgeSAM-10x	10% SA-1B	43.0	30.3	48.9	55.1	22.1	9.6	38.7	164.3	-

A. More Quantitative Results

In our main paper, we compare our method with SAM [23] and MobileSAM [58]. Here, we supplement more results compared to a recent work, FastSAM [65]. Different from MobileSAM and EdgeSAM, FastSAM does not follow the encoder-decoder architecture of SAM. Instead, it yields masks of all the instances and selects the object of interest through post-prediction handcrafted rules. As a result, the prompts are not considered during the mask prediction, which limits the flexibility of the outputs. Following the experiment setting of FastSAM, we measure the Average Precision (AP) on the COCO dataset [28] using ViTDet-H [27] as the detector, which provides boxes and class labels. Here, we do not apply an additional mask refinement iteration per the setting of the original SAM paper [23], so the numbers are slightly worse than what is reported in SAM. Note that ViTDet-H is much stronger than the detector that we use in the main paper (box AP: 58.7 vs. 47.4). In addition, FastSAM is trained with 2% images of SA-1B, which is twice as many as both MobileSAM and EdgeSAM. As shown in Tab. 6, EdgeSAM consistently surpasses FastSAM and MobileSAM by a considerate margin but still falls behind the original SAM. Tab. 6 also shows that, with more training data, EdgeSAM can achieve better performance, especially for large objects. Besides, when it comes to efficiency, EdgeSAM achieves the best results, being significantly faster than all its counterparts, in particular, on edge devices, such as iPhone 14.

B. More Ablation Studies

Training Datasets. In our default setting, we train EdgeSAM with 1% images of the SA-1B [23] dataset. In Tab. 7a, we study the impact of training datasets on transferability. In specific, we keep the model and training pipeline the same while switching the training dataset among 1% SA-1B, COCO [28], and LVIS [11]. Note that all datasets contain a similar number of images (approximately 110K).

Results show that training with SA-1B archives the best performance across all test sets with box prompts, while with point prompts, training and testing in the same domain yield the best result. This suggests that with informative prompts, such as boxes, distillation on the SA-1B dataset is sufficient for zero-shot transfer. However, with ambiguous prompts, such as a single point, efforts need to be made to capture the granularity priors of the testing datasets. This motivates us to leverage an additional RPN to explicitly capture such priors.

Training Losses for Decoder. In our main paper, we mention that supervising the student with teacher mask output as the ground truth is the most effective for decoder loss. Here, we provide more details of our empirical findings. In particular, we compare various configurations, including (1) combining mask loss with aligning attention maps from the teacher and student decoder; (2) combining mask loss with aligning the IoU predictions between teacher and student; (3) aligning the output feature maps between the teacher and student decoder. As shown in Tab. 7b, the plain mask loss supervision yields the best performance. Thus, instead of exploring different loss combinations, we turn to study the strategy to select the proper prompts during distillation and further propose the prompt-in-the-loop distillation.

Number of Prompts. Given that each sample of SA-1B contains around 100 instances, training all of them in a single batch causes VRAM overflow. Therefore, we randomly sample a subset for each iteration. In Tab. 7c, we study the impact of the number of prompts for sampling and find that 16 prompts achieve the best trade-off. Thus, we set it as the default.

C. Qualitative Results Compared with SAM

In Fig. 6, we provide more qualitative results of EdgeSAM and compare it with the original SAM under single point, box, and everything mode. Note that since EdgeSAM follows the same encoder-decoder architecture as SAM, everything mode is costly. Specifically, in everything mode,

Table 7. **More ablation studies.** Box and center denote testing EdgeSAM with GT-box and center of the GT-mask as the prompt respectively. COCO mAP and boundary IoU [8] are obtained with the Detic [66] object detector providing box prompts and class labels (box mAP 47.4). Note that, for all the ablations, we set the number of prompt sampling loops to 0 (no re-sampling). SA-1B* means 1% SA-1B. **Bold** font indicates the best number and the default configuration we adopt.

(a) **Training datasets.**

Dataset	SA-1K		COCO		LVIS	
	Box	Center	Box	Center	Box	Center
SA-1B*	83.1	67.4	76.7	48.2	76.1	53.5
COCO	81.3	63.1	76.1	50.8	74.7	54.2
LVIS	82.4	63.6	75.7	50.2	75.4	54.9

(b) **Decoder losses.**

Method	SA-1K		COCO	
	Box	Center	AP	BIoU
Mask	83.1	67.4	35.1	22.4
Mask + Attn.	82.8	67.0	35.0	22.3
Mask + IoU	82.5	67.1	34.9	22.2
Img. Feat.	71.6	55.0	30.2	17.2

(c) **Number of prompts.** In this ablation, we freeze the mask decoder of EdgeSAM.

#Prompt	SA-1K		COCO	
	Box	Center	AP	BIoU
8	83.6	67.6	34.3	21.7
16	83.5	67.7	34.6	21.9
32	83.6	67.6	34.3	21.6

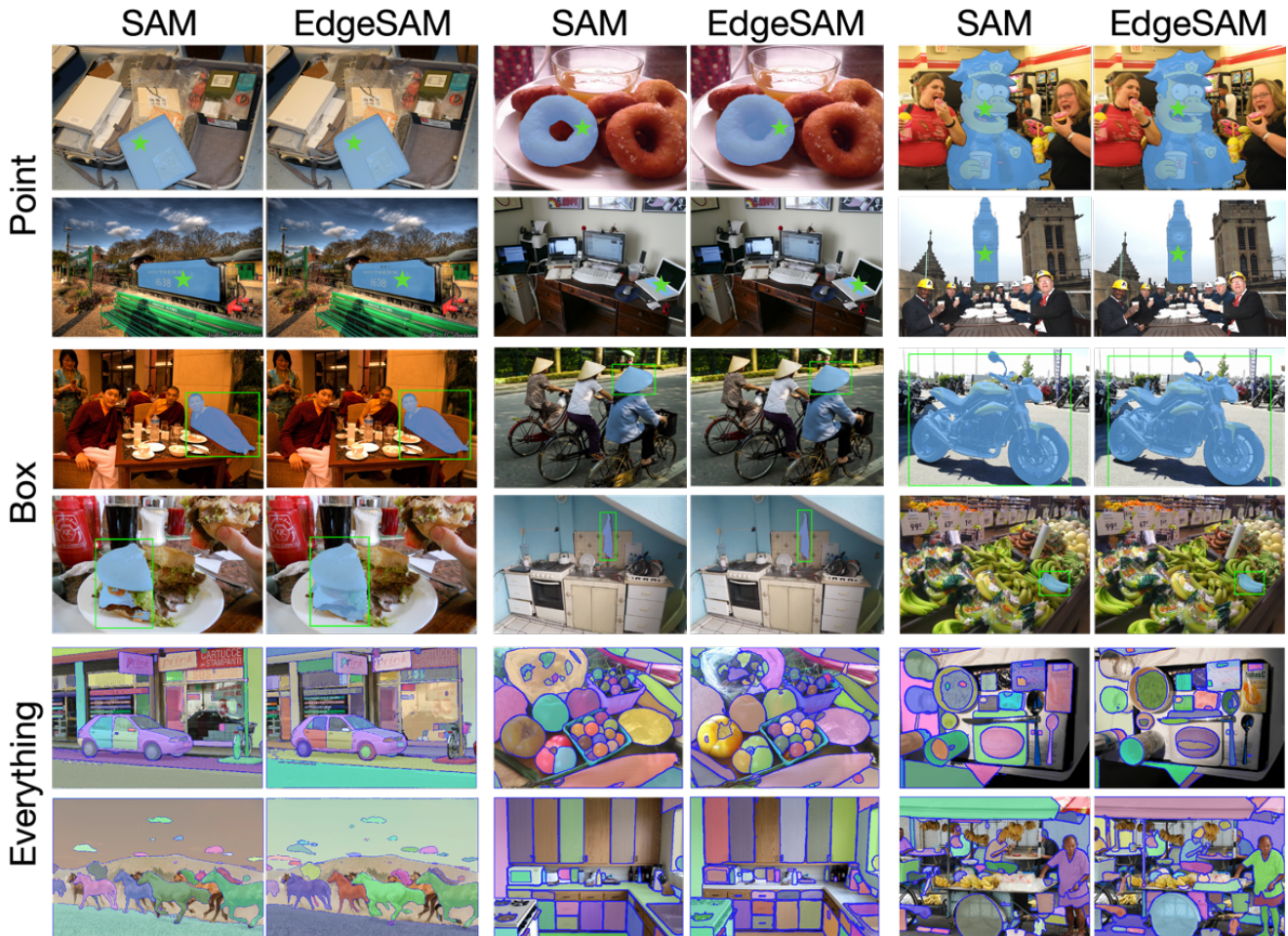


Figure 6. **Qualitative results of EdgeSAM and SAM under point, box, and everything mode.**

points in a 32×32 grid are fed to the decoder, which results in 1,024 times decoder inference. As EdgeSAM is built for inference-speed-sensitive devices, we do not advocate for using the everything mode of EdgeSAM in practice. Therefore, we provide visualization examples mainly to discuss its behavior compared to SAM. As expected, the overall mask quality of EdgeSAM is inferior to SAM, but they are comparable, especially for box prompts. One common failure case for EdgeSAM is mis-segmenting the holes within an object, for instance, the donut example in Fig. 6 (row 1, col 4). We think this might be due to the lack of training samples. But in actual use, one can add a negative point in the hole area to explicitly force EdgeSAM to exclude such regions. Moreover, in everything mode, only masks with confident scores over a certain threshold are kept. Thus, regions without masks indicate unsatisfactory mask predictions. Same as SAM, EdgeSAM covers most objects in the scene, which demonstrates its capability.

References

- [1] Daniel Bolya, Chong Zhou, Fanyi Xiao, and Yong Jae Lee. Yolact: Real-time instance segmentation. In *ICCV*, 2019. 2
- [2] Han Cai, Junyan Li, Muyan Hu, Chuang Gan, and Song Han. Efficientvit: Lightweight multi-scale attention for on-device semantic segmentation. In *ICCV*, 2023. 3, 7
- [3] Nicolas Carion, Francisco Massa, Gabriel Synnaeve, Nicolas Usunier, Alexander Kirillov, and Sergey Zagoruyko. End-to-end object detection with transformers. In *ECCV*, 2020. 2
- [4] Jiahao Chang, Shuo Wang, Hai-Ming Xu, Zehui Chen, Chenhongyi Yang, and Feng Zhao. Detrdistill: A universal knowledge distillation framework for detr-families. In *ICCV*, 2023. 1, 2
- [5] Kai Chen, Jiaqi Wang, Jiangmiao Pang, Yuhang Cao, Yu Xiong, Xiaoxiao Li, Shuyang Sun, Wansen Feng, Ziwei Liu, Jiarui Xu, et al. Mmdetection: Open mmlab detection toolbox and benchmark. *arXiv preprint*, 2019. 6
- [6] Xiaokang Chen, Jiahui Chen, Yan Liu, and Gang Zeng. D3etr: Decoder distillation for detection transformer. *arXiv preprint*, 2022. 1, 2
- [7] Yinpeng Chen, Xiyang Dai, Dongdong Chen, Mengchen Liu, Xiaoyi Dong, Lu Yuan, and Zicheng Liu. Mobileformer: Bridging mobilenet and transformer. In *CVPR*, 2022. 2
- [8] Bowen Cheng, Ross Girshick, Piotr Dollár, Alexander C Berg, and Alexander Kirillov. Boundary iou: Improving object-centric image segmentation evaluation. In *CVPR*, 2021. 5, 6, 10
- [9] Marco Forte, Brian Price, Scott Cohen, Ning Xu, and François Pitié. Getting to 99% accuracy in interactive segmentation. *arXiv preprint*, 2020. 4
- [10] Yushuo Guan, Pengyu Zhao, Bingxuan Wang, Yuanxing Zhang, Cong Yao, Kaigui Bian, and Jian Tang. Differentiable feature aggregation search for knowledge distillation. In *ECCV*, 2020. 2
- [11] Agrim Gupta, Piotr Dollar, and Ross Girshick. Lvis: A dataset for large vocabulary instance segmentation. In *CVPR*, 2019. 2, 3, 5, 9
- [12] Kai Han, Yunhe Wang, Qi Tian, Jianyuan Guo, Chunjing Xu, and Chang Xu. Ghostnet: More features from cheap operations. In *CVPR*, 2020. 2
- [13] Geoffrey Hinton, Oriol Vinyals, and Jeff Dean. Distilling the knowledge in a neural network. *NeurIPS*, 2014. 2
- [14] Weixiang Hong, Qingpei Guo, Wei Zhang, Jingdong Chen, and Wei Chu. Lpsnet: A lightweight solution for fast panoptic segmentation. In *CVPR*, 2021. 2
- [15] Yuanduo Hong, Huihui Pan, Weichao Sun, and Yisong Jia. Deep dual-resolution networks for real-time and accurate semantic segmentation of road scenes. *arXiv preprint*, 2021. 2
- [16] Andrew Howard, Mark Sandler, Grace Chu, Liang-Chieh Chen, Bo Chen, Mingxing Tan, Weijun Wang, Yukun Zhu, Ruoming Pang, Vijay Vasudevan, et al. Searching for mobilenetv3. In *ICCV*, 2019. 2
- [17] Andrew G Howard, Menglong Zhu, Bo Chen, Dmitry Kalenichenko, Weijun Wang, Tobias Weyand, Marco Andreetto, and Hartwig Adam. Mobilenets: Efficient convolutional neural networks for mobile vision applications. *arXiv preprint*, 2017. 2
- [18] Edward J Hu, Yelong Shen, Phillip Wallis, Zeyuan Allen-Zhu, Yuanzhi Li, Shean Wang, Lu Wang, and Weizhu Chen. Lora: Low-rank adaptation of large language models. In *ICLR*, 2022. 4, 7
- [19] Jie Hu, Linyan Huang, Tianhe Ren, Shengchuan Zhang, Rongrong Ji, and Liujuan Cao. You only segment once: Towards real-time panoptic segmentation. In *CVPR*, 2023. 2
- [20] Linjiang Huang, Kaixin Lu, Guanglu Song, Liang Wang, Si Liu, Yu Liu, and Hongsheng Li. Teach-detr: Better training detr with teachers. *arXiv preprint*, 2022. 1, 2
- [21] Peter J Huber. Robust estimation of a location parameter. In *Breakthroughs in statistics: Methodology and distribution*. 1992. 5
- [22] Forrest N Iandola, Song Han, Matthew W Moskewicz, Khalid Ashraf, William J Dally, and Kurt Keutzer. Squeezenet: Alexnet-level accuracy with 50x fewer parameters and 0.5 mb model size. *arXiv preprint*, 2016. 2
- [23] Alexander Kirillov, Eric Mintun, Nikhila Ravi, Hanzi Mao, Chloe Rolland, Laura Gustafson, Tete Xiao, Spencer Whitehead, Alexander C Berg, Wan-Yen Lo, et al. Segment anything. *ICCV*, 2023. 1, 2, 5, 9
- [24] Jiashi Li, Xin Xia, Wei Li, Huixia Li, Xing Wang, Xuefeng Xiao, Rui Wang, Min Zheng, and Xin Pan. Next-vit: Next generation vision transformer for efficient deployment in realistic industrial scenarios. *arXiv preprint*, 2022. 2
- [25] Xiangtai Li, Ansheng You, Zeping Zhu, Houlong Zhao, Maoke Yang, Kuiyuan Yang, and Yunhai Tong. Semantic flow for fast and accurate scene parsing. In *ECCV*, 2020. 2
- [26] Xiangtai Li, Jiangning Zhang, Yibo Yang, Guangliang Cheng, Kuiyuan Yang, Yu Tong, and Dacheng Tao. Sfnets: Faster and accurate semantic segmentation via semantic flow. *IJCV*, 2023. 2

- [27] Yanghao Li, Hanzi Mao, Ross Girshick, and Kaiming He. Exploring plain vision transformer backbones for object detection. In *ECCV*, 2022. 3, 9
- [28] Tsung-Yi Lin, Michael Maire, Serge Belongie, James Hays, Pietro Perona, Deva Ramanan, Piotr Dollár, and C Lawrence Zitnick. Microsoft coco: Common objects in context. In *ECCV*, 2014. 1, 2, 3, 5, 6, 9
- [29] Tsung-Yi Lin, Piotr Dollár, Ross Girshick, Kaiming He, Bharath Hariharan, and Serge Belongie. Feature pyramid networks for object detection. In *CVPR*, 2017. 3, 5, 7
- [30] Tsung-Yi Lin, Priya Goyal, Ross Girshick, Kaiming He, and Piotr Dollár. Focal loss for dense object detection. In *ICCV*, 2017. 5
- [31] Yifan Liu, Ke Chen, Chris Liu, Zengchang Qin, Zhenbo Luo, and Jingdong Wang. Structured knowledge distillation for semantic segmentation. In *CVPR*, 2019. 1, 2, 3, 7, 8
- [32] Ilya Loshchilov and Frank Hutter. Decoupled weight decay regularization. In *ICLR*, 2019. 5
- [33] Hailong Ma, Xin Xia, Xing Wang, Xuefeng Xiao, Jiashi Li, and Min Zheng. MocoVIT: Mobile convolutional vision transformer. *arXiv preprint*, 2022. 2
- [34] Ningning Ma, Xiangyu Zhang, Hai-Tao Zheng, and Jian Sun. ShuffleNet v2: Practical guidelines for efficient CNN architecture design. In *ECCV*, 2018. 2
- [35] Muhammad Maaz, Abdelrahman Shaker, Hisham Cholakkal, Salman Khan, Syed Waqas Zamir, Rao Muhammad Anwer, and Fahad Shahbaz Khan. Edgenext: efficiently amalgamated CNN-transformer architecture for mobile vision applications. In *ECCVW*, 2022. 2
- [36] Sachin Mehta and Mohammad Rastegari. Mobilevit: Lightweight, general-purpose, and mobile-friendly vision transformer. In *ICLR*, 2022. 2
- [37] Sachin Mehta, Mohammad Rastegari, Anat Caspi, Linda Shapiro, and Hannaneh Hajishirzi. Espnet: Efficient spatial pyramid of dilated convolutions for semantic segmentation. In *ECCV*, 2018. 2
- [38] Sachin Mehta, Mohammad Rastegari, Linda Shapiro, and Hannaneh Hajishirzi. Espnetv2: A light-weight, power efficient, and general purpose convolutional neural network. In *CVPR*, 2019. 2
- [39] Junting Pan, Adrian Bulat, Fuwen Tan, Xiatian Zhu, Lukasz Dudziak, Hongsheng Li, Georgios Tzimiropoulos, and Brais Martinez. Edgevits: Competing light-weight CNNs on mobile devices with vision transformers. In *ECCV*, 2022. 2
- [40] Alec Radford, Jong Wook Kim, Chris Hallacy, Aditya Ramesh, Gabriel Goh, Sandhini Agarwal, Girish Sastry, Amanda Askell, Pamela Mishkin, Jack Clark, et al. Learning transferable visual models from natural language supervision. In *ICML*, 2021. 3
- [41] Shaoqing Ren, Kaiming He, Ross Girshick, and Jian Sun. Faster r-cnn: Towards real-time object detection with region proposal networks. *NeurIPS*, 2015. 5
- [42] Mark Sandler, Andrew Howard, Menglong Zhu, Andrey Zhmoginov, and Liang-Chieh Chen. Mobilenetv2: Inverted residuals and linear bottlenecks. In *CVPR*, 2018. 2
- [43] Changyong Shu, Yifan Liu, Jianfei Gao, Zheng Yan, and Chunhua Shen. Channel-wise knowledge distillation for dense prediction. In *ICCV*, 2021. 1, 2, 3, 7, 8
- [44] Konstantin Sofiiuk, Ilya A Petrov, and Anton Konushin. Reviving iterative training with mask guidance for interactive segmentation. In *ICIP*, 2022. 4
- [45] Carole H Sudre, Wenqi Li, Tom Vercauteren, Sebastien Ourselin, and M Jorge Cardoso. Generalised dice overlap as a deep learning loss function for highly unbalanced segmentations. In *MICCAI*, 2017. 4
- [46] Mingxing Tan, Ruoming Pang, and Quoc V Le. Efficientdet: Scalable and efficient object detection. In *CVPR*, 2020. 5
- [47] Matthew Tancik, Pratul Srinivasan, Ben Mildenhall, Sara Fridovich-Keil, Nithin Raghavan, Utkarsh Singhal, Ravi Ramamoorthi, Jonathan Barron, and Ren Ng. Fourier features let networks learn high frequency functions in low dimensional domains. *NeurIPS*, 2020. 3
- [48] Qiang Wan, Zilong Huang, Jiachen Lu, Gang Yu, and Li Zhang. Seaformer: Squeeze-enhanced axial transformer for mobile semantic segmentation. In *ICLR*, 2023. 2
- [49] Ao Wang, Hui Chen, Zijia Lin, Hengjun Pu, and Guiguang Ding. Repvit: Revisiting mobile CNN from ViT perspective. *arXiv preprint*, 2023. 2, 3, 7
- [50] Tao Wang, Li Yuan, Xiaopeng Zhang, and Jiashi Feng. Distilling object detectors with fine-grained feature imitation. In *CVPR*, 2019. 2
- [51] Yukang Wang, Wei Zhou, Tao Jiang, Xiang Bai, and Yongchao Xu. Intra-class feature variation distillation for semantic segmentation. In *ECCV*, 2020. 2
- [52] Kan Wu, Jinnian Zhang, Houwen Peng, Mengchen Liu, Bin Xiao, Jianlong Fu, and Lu Yuan. Tinyvit: Fast pretraining distillation for small vision transformers. In *ECCV*, 2022. 3, 7
- [53] Jiafeng Xie, Bing Shuai, Jian-Fang Hu, Jingyang Lin, and Wei-Shi Zheng. Improving fast segmentation with teacher-student learning. *BMVC*, 2018. 2
- [54] Qizhe Xie, Minh-Thang Luong, Eduard Hovy, and Quoc V Le. Self-training with noisy student improves imagenet classification. In *CVPR*, 2020. 2
- [55] Changqian Yu, Jingbo Wang, Chao Peng, Changxin Gao, Gang Yu, and Nong Sang. Bisenet: Bilateral segmentation network for real-time semantic segmentation. In *ECCV*, 2018. 2
- [56] Changqian Yu, Changxin Gao, Jingbo Wang, Gang Yu, Chunhua Shen, and Nong Sang. Bisenet v2: Bilateral network with guided aggregation for real-time semantic segmentation. *IJCV*, 2021. 2
- [57] Li Yuan, Francis EH Tay, Guilin Li, Tao Wang, and Jiashi Feng. Revisiting knowledge distillation via label smoothing regularization. In *CVPR*, 2020. 2
- [58] Chaoning Zhang, Dongshen Han, Yu Qiao, Jung Uk Kim, Sung-Ho Bae, Seungkyu Lee, and Choong Seon Hong. Faster segment anything: Towards lightweight SAM for mobile applications. *arXiv preprint*, 2023. 1, 2, 3, 5, 9
- [59] Jiangning Zhang, Xiangtai Li, Jian Li, Liang Liu, Zhucun Xue, Boshen Zhang, Zhengkai Jiang, Tianxin Huang, Yabiao Wang, and Chengjie Wang. Rethinking mobile block for efficient attention-based models. In *ICCV*, 2023. 2
- [60] Linfeng Zhang and Kaisheng Ma. Improve object detection with feature-based knowledge distillation: Towards accurate and efficient detectors. In *ICLR*, 2020. 2

- [61] Wenqiang Zhang, Zilong Huang, Guozhong Luo, Tao Chen, Xinggang Wang, Wenyu Liu, Gang Yu, and Chunhua Shen. Topformer: Token pyramid transformer for mobile semantic segmentation. In *CVPR*, 2022. [2](#)
- [62] Xiangyu Zhang, Xinyu Zhou, Mengxiao Lin, and Jian Sun. Shufflenet: An extremely efficient convolutional neural network for mobile devices. In *CVPR*, 2018. [2](#)
- [63] Zizhao Zhang, Han Zhang, Sercan O Arik, Honglak Lee, and Tomas Pfister. Distilling effective supervision from severe label noise. In *CVPR*, 2020. [2](#)
- [64] Hengshuang Zhao, Xiaojuan Qi, Xiaoyong Shen, Jianping Shi, and Jiaya Jia. Icnet for real-time semantic segmentation on high-resolution images. In *ECCV*, 2018. [2](#)
- [65] Xu Zhao, Wenchao Ding, Yongqi An, Yinglong Du, Tao Yu, Min Li, Ming Tang, and Jinqiao Wang. Fast segment anything. *arXiv preprint*, 2023. [2](#), [9](#)
- [66] Xingyi Zhou, Rohit Girdhar, Armand Joulin, Philipp Krähenbühl, and Ishan Misra. Detecting twenty-thousand classes using image-level supervision. In *ECCV*, 2022. [6](#), [10](#)